Extreme Mechanics Letters 23 (2018) 17–23

Contents lists available at ScienceDirect

Extreme Mechanics Letters

journal homepage: www.elsevier.com/locate/eml

Extreme mechanics in laminated shells: New insights

R.M.J. Groh *, A. Pirrera

Bristol Composites Institute (ACCIS), University of Bristol, Queen's Building, University Walk, Bristol, BS8 1TR, UK

ARTICLE INFO

Article history:
Received 19 June 2018
Received in revised form 19 July 2018
Accepted 19 July 2018
Available online 21 July 2018

Keywords:
Nonlinear structures
Bifurcations
Morphing
Composite material

ABSTRACT

Fibre-reinforced composite laminates are increasingly popular for lightweight applications in the aerospace, wind turbine and automotive industries. Apart from their excellent specific strength and stiffness properties, their orthotropic and layered construction can be exploited to create bistable systems that are useful for shape-adaptive morphing or energy-harvesting applications. The nonlinear interaction between initial curvature and induced thermal stresses can lead to "extreme" mechanics with rich branching and multi-stable behaviour. Here, we explore the multi-stability of curved composite laminates in the two-dimensional parameter space of temperature and mechanical loading. Analyses conducted via finite element discretisation and numerical continuation algorithms reveal possible snapping behaviour between five different mode shapes for different combinations of applied load and temperature. Furthermore, we show that a composite laminate can exhibit four stable, self-equilibrated mode shapes for a narrow temperature range. Hence, the multi-stable and nonlinear mechanics of composite laminates is much more complex than previously assumed, and this may influence the design of more versatile morphing structures.

1. Introduction

In structural engineering, elastic instabilities are historically viewed as a "failure" mechanism. An alternative perspective has developed over the last decade, whereby instabilities are used for additional functionality [1]. Example applications include energy harvesting [2,3], reversible shape-adaptation [4,5], surface texturing [6], actuation [7], self-encapsulation [8], auxetic materials [9] and energy dissipation [10].

In many of these applications, the underlying mechanical principle is multi-stability. Multi-stability often arises in geometrically curved structures in a stress-free state – *e.g.* a circular arch snapped between two inverted shapes – or alternatively, in curved geometries obtained from an induced stress field—*e.g.* the post-buckled state of the slender elastica. In the latter case, geometry and pre-stress can interact nonlinearly to produce very rich and oftentimes complex bifurcation behaviour, a classical example being the post-buckling response of the axially compressed cylinder [11]. Although this rich bifurcation behaviour can broaden the spectrum of potentially useful functionality, there are still open research questions to how this behaviour is best explored numerically [12], validated experimentally [13], and reliably controlled in practice [14].

Modern composite materials, such as carbon-fibre and fibre-glass laminates, are a natural source of complex bifurcation behaviour and interesting "extreme" mechanics. Composite laminates are often manufactured by stacking plies of fibre-reinforced plastic on a mould surface in a specific sequence. Although reinforced plastics with curvilinear fibres exist [15], traditionally the reinforcing fibres are straight and point in a specific direction, θ, with respect to a defined material axis. In this manner, a composite laminate can be assembled from individual composite layers with different fibre orientations, and the assembly then cured under elevated temperature and pressure. As long as the resin that binds fibres together is free to flow during cure, it can be assumed that the cured composite takes a stress-free condition at its elevated curing temperature. Upon cooling to room temperature, which is typically a ΔT in the region of $[-200, -160]$ K, thermally induced shrinkage is induced. Due to the orthotropy of fibre-reinforced plastics, each layer will want to contract/expand by different amounts and in different directions. However, the restraint enforced by polymer bonding between layers induces intralaminar tensile/compressive stresses. If the lamination sequence is symmetric – hence, for every θ-fibre orientation below the mid-surface of the laminate there exists a symmetric θ-layer above the laminate mid-surface – then the bending moments induced by these thermal stresses will balance about the mid-surface, and the laminate will retain the stress-free curvature. If the lamination sequence is non-symmetric,

* Corresponding author.
E-mail address: rainer.groh@bristol.ac.uk (R.M.J. Groh).

https://doi.org/10.1016/j.eml.2018.07.004

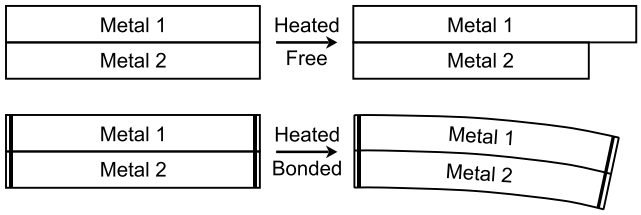

Fig. 1. The ubiquitous bimetallic strip.

then a thermal bending moment is induced that warps the laminate. In this sense, a non-symmetric composite laminate is a two-dimensional extension of the ubiquitous bimetallic strip shown in Fig. 1.

As a non-symmetric composite laminate cools to room temperature, *i.e.* upon warping, it may "morph" onto different shapes as a result of symmetry-breaking bifurcations. As a direct result of energy minimisation, flat laminates, for instance, may transition from energetically expensive membrane-dominated configurations of non-zero Gaussian curvature, to more favourable bending-dominated cylindrical shapes [16]. Such cylindrical laminates are bistable, meaning they can be snapped from one cylindrical shape to an inverted second cylindrical shape. For initially curved panels, tristable configurations are also possible [17]. Hence, the nonlinear interaction of interlayer constraints, differential free thermal strains and initially curved geometries can lead to a plethora of different multi-stable solutions and snap-through events depending on the particular laminate configuration.

Multi-stable composite laminates are particularly attractive for aerospace applications because they are lightweight and a potential mechanism for aerodynamic morphing [18]. In the past, the development of quantitative and qualitative models has focused on specialised methods tailored to simple geometries and boundary conditions [19–22]. Alternatively, commercial finite element packages have been used [17,23]. In both cases, the solution of the nonlinear boundary value problem is typically restricted to the simplest path-following techniques, without recourse to direct computation of branch points, robust algorithms for branch-switching, or bifurcation tracking through parameter space. As a result, much of the non-intuitive bifurcation behaviour remains unexplored.

The purpose of this paper is, therefore, to revisit two classic morphing problems in the literature [22,24], and by means of more general numerical continuation procedures, to demonstrate additional interesting solutions and shape changes that can occur in parameter space. Section 2 briefly defines the problem and the model used to analyse it. The results for the two cylindrical laminates considered are discussed in Section 3 and conclusions are drawn in Section 4.

2. Problem definition and modelling technique

Consider the thin, cylindrical shell section drawn schematically in Fig. 2. The radius of the shell is $R = 500$ mm with straight longitudinal edges of length L and curved lateral edges of equal arc-length $W = 250$ mm. Two different lengths, L, will be considered in this paper—one of square planform with $L = 250$ mm and one of rectangular planform with $L = 500$ mm. These two shells are henceforth denoted as the "square" and "rectangular" shell, respectively.

This cylindrical section is used as a tool surface to manufacture a laminated composite panel with layer properties given in Table 1. Each ply has a thickness of 0.131 mm and the material axis is defined to be parallel to the x-axis in Fig. 2. With respect to this

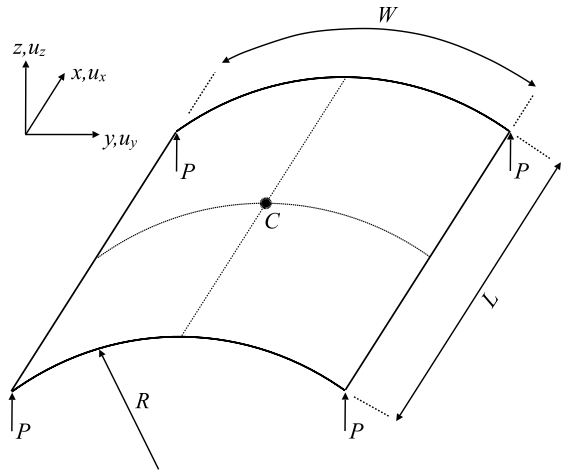

Fig. 2. A cylindrical tool plate used during laminate curing. The imposed boundary conditions at mid-point C and applied corner loads P refer to post-cure loading once the laminate has been removed from the tool plate.

material axis, the square and rectangular shell have a stacking sequence of $\theta = [90_2/0_2]$ and $\theta = [0_2/90_2]$, respectively, layered from bottom-up in the direction of the radius of curvature shown in Fig. 2.

Once the laminate is removed from the tool plate, we model its cool-down from the cure temperature of 473 K to room temperature at 293 K, by clamping the laminate at its midpoint C and applying a uniform temperature change throughout the shell domain. For some temperatures, the laminate can be snapped between different states by applying a transverse point load P at its four corners.

In the applied mathematics community, the methods of multi-parameter analysis, branch-switching and bifurcation tracking are well established [25–27]. However, these techniques are seldom used in quasi-static mechanics applications, where specialised arc-length techniques restricted to a single parameter – the applied load – are predominantly used [28]. The application of broader numerical continuation methods within implicit, quasi-static finite element solvers often go by the name of "generalised path-following" and it is such a framework that we use herein (see Ref. [12] for the detailed formulation). The generalised path-following technique allows us to quasi-statically follow stable and unstable equilibria; branch-switch to additional solutions at critical points, if these exist; and efficiently trace critical points with respect to an additional parameter (*e.g.* geometry, material properties, second force, *etc.*).

Throughout this work we use so-called "degenerated shell elements" [29] based on the assumptions of first-order shear deformation theory [30] (shear correction factor $k = 5/6$) formulated using the full Green–Lagrange strain tensor and a total Lagrangian reference system. The square shell is discretised into a 43×43 node mesh of 196 fully integrated, 16-node shell elements using the shell director parametrisation of Ramm [31] (two rotations per node, no drilling around the shell director). For the rectangular shell, the mesh was refined to 43 nodes in the curved direction and 85 nodes in the longitudinal direction (392 elements). The effects of shear and membrane locking are minimised by using bi-cubic isoparametric interpolation functions, and by refining the mesh sufficiently until convergence with respect to a 50×50 element converged mesh of reduced integration S4R elements of the commercial finite element software ABAQUS is obtained [22].

Table 1
Orthotropic material properties used for the layered shell, where the 1-direction points along the fibres, the 2-direction is perpendicular to the fibres, and the 3-direction is normal to the orthotropic layer.

E_{11} (GPa)	E_{22} (GPa)	ν_{12} (-)	G_{12} (GPa)	G_{23} (GPa)	G_{13} (GPa)	α_{11} (1/K)	α_{22} (1/K)
161	11.38	0.32	5.17	5.17	5.17	-1.8×10^{-8}	3.0×10^{-5}

3. Results

The analysis of the square (Section 3.1) and rectangular (Section 3.2) shells follows the same basic recipe. First, the laminates are cooled through a temperature differential of $\Delta T = -180\,\mathrm{K}$ to reveal stable solutions in the self-equilibrated state of no applied mechanical load ($P = 0$). By branch-switching at pitchfork bifurcations, symmetry-breaking equilibria in the self-equilibrated parameter space can be identified, and in this manner, additional stable solutions are observed. Second, at any point throughout the temperature range an external mechanical load ($P \neq 0$) can be applied to snap the shell between different equilibrium states, when these exist. This analysis reveals further stable equilibria, which, although not self-equilibrated, nevertheless enable snapping between two shapes at non-zero load.

In all equilibrium manifolds shown henceforth, blue segments denote statically stable equilibria and red curves denote statically unstable equilibria. Black dots are used to denote singular points (limit or branching points), whilst loci of singular points with respect to two simultaneously varying parameters are traced as black curves.

3.1. Square shell

Fig. 3 shows the cooling behaviour of the square shell in terms of the temperature differential from curing (ΔT) *vs* the shell-corner deflection in the z-direction (u_z) in the z-direction defined in Fig. 2. When the laminate comes off the tool plate, it is in the cylindrical shape of mode O, and remains so until reaching a branch point at $\Delta T = -9.79\,\mathrm{K}$. At this symmetry-breaking bifurcation, the original cylindrical shape becomes unstable and the shell transitions into one of two twisted modes (I and II) shown in Fig. 3 and observed experimentally by Eckstein et al. [24]. These twisted modes connect back to a cylindrical solution at branch point $\Delta T = -31.5\,\mathrm{K}$. The existence of two separate, self-equilibrated twisting modes indicates that the shell is bistable within the parameter range $\Delta T = [-31.5, -9.79]\,\mathrm{K}$ and, as will be shown later, can be snapped between these two states by the application of corner forces P. As illustrated by mode III in Fig. 3, the cylindrical shape for $\Delta T < -31.5\,\mathrm{K}$ is rotated by 90 deg compared to the original tool plate mode O (*i.e.* the curvature moves from the y-axis to the x-axis), and the twisting modes I and II therefore create connections between these two cylindrical shapes. As the laminate cools further, the curvature of mode III increases until it reaches the cylindrical shape at room temperature ($\Delta T = -180\,\mathrm{K}$) shown in Fig. 3.

The addition of initial curvature therefore allows bifurcations to additional states beyond the classically observed saddle-to-cylindrical bifurcations of initially flat plates [32]. Twisted states have been observed by cooling initially flat laminates with fibre angles at an angle to the geometric axes [33], or indeed by cutting differentially pre-stressed bi-layers at an angle to the pre-stressing direction [34]. Here, however, the twisting mode arises because of a symmetry-breaking bifurcation that causes the shell to deform at an angle to the cooling forces, in the same way that an arch may snap-through *asymmetrically* even when loaded *symmetrically*. For a $[90_2/0_2]$ layup, the temperature gradient decreases the initial curvature and introduces curvature in the originally straight direction, thereby rotating the initial curvature through 90 deg. The energetically most favourable way of accomplishing this transition

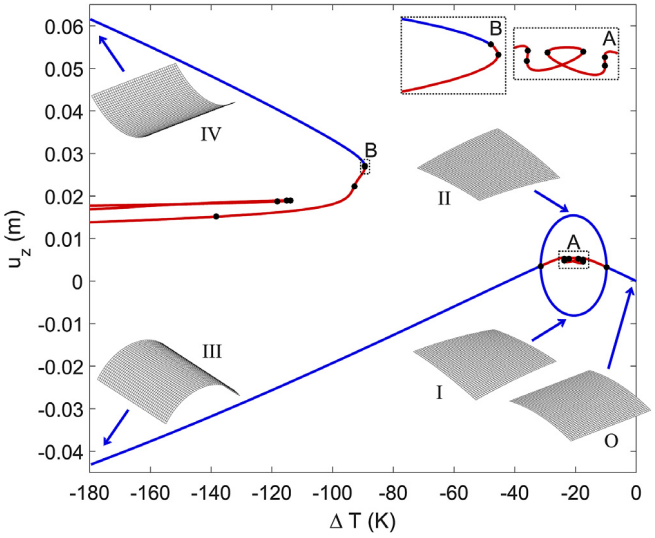

Fig. 3. Broken pitchfork diagram showing the cooling behaviour of a cylindrically cured cross-ply laminate $[90_2/0_2]$ with mode shapes shown at different points throughout the cooling temperature range.

for the current degree of initial curvature is via a gradual twisting transition. However, previous work by the present authors has demonstrated that the twisting mode vanishes once the initial curvature falls beneath a critical threshold (see Fig. 8c in Ref. [12]).

The primary cooling branch is part of a more complex equilibrium manifold. For example, the laminate can be snapped into an inverted and 90 deg-rotated cylindrical shape IV shown at $\Delta T = -180\,\mathrm{K}$ in Fig. 3. This additional stable equilibrium forms the broken-away part of the fundamental broken pitchfork and exist for $\Delta T < -89.4\,\mathrm{K}$. In summary, the composite laminate loses its self-equilibrated bistability in the range $\Delta T = [-89.4, -31.5]\,\mathrm{K}$. The broken-away stable mode of a broken pitchfork typically loses stability at a limit point, but as shown in inset B of Fig. 3, a symmetry-breaking branching point just precedes the limit point, such that the cylindrical mode IV loses stability there. Two additional branching points exist on the subsequent unstable portion of the broken-away manifold, but the equilibria branching from these two singular points are always unstable, and for clarity and simplicity, not shown here. Another unusual feature of this broken pitchfork in Fig. 3 is a second, smaller broken-away manifold for $\Delta T < -113.8\,\mathrm{K}$ with additional branching points (further branches not shown for clarity), further illustrating the rich nonlinear behaviour of composite laminates, which may go undetected without the requisite computational means.

Fig. 4a shows the snap-through manifold of corner force P *vs* corner displacement u_z at room temperature—hence snapping from one cylindrical shape to the other. The load–displacement curve takes the typical sigmoidal curve created by two back-to-back limit points. However, counter to what is often assumed in the composite morphing literature, the laminate loses stability and snaps-through at a symmetry-breaking subcritical branching point and not at the limit point (maximum P). The snap-back point, however, takes the form of the usual limit point (minimum). Fig. 4a also shows a black foldline that tracks the evolution of the limit

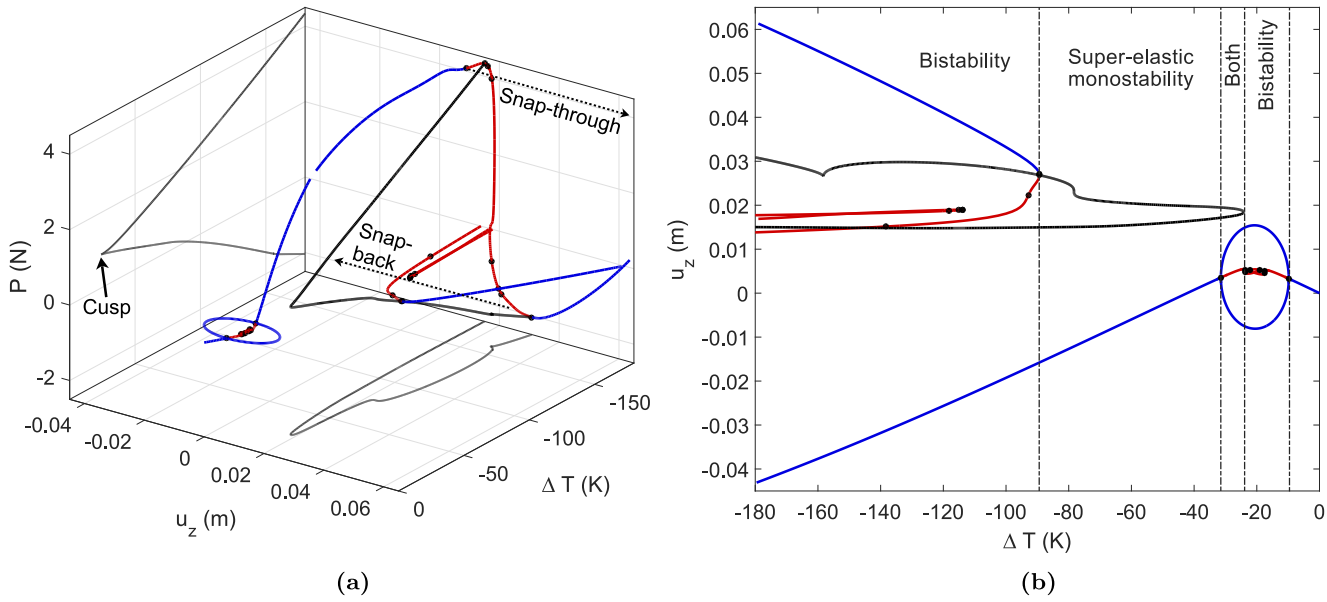

Fig. 4. (a) 3-D view of the snap-through manifold at room temperature ($\Delta T = -180$ K) from one cylindrical mode to another via the application of corner forces P, superimposed on the broken-pitchfork manifold for $P = 0$. The black curve traces the evolution of the maximum and minimum limit points on the snap-through manifold in u_z-ΔT-P space. Orthonormal projections of the foldline on the P-ΔT and u_z-ΔT planes are also shown. (b) The broken-pitchfork manifold for $P = 0$ with the orthonormal projection of the foldline. The plot is split into different regions that correspond to the taxonomy of nonlinear snapping behaviour classified by Danso & Karpov [35]. (For interpretation of the references to colour in this figure legend, the reader is referred to the web version of this article.)

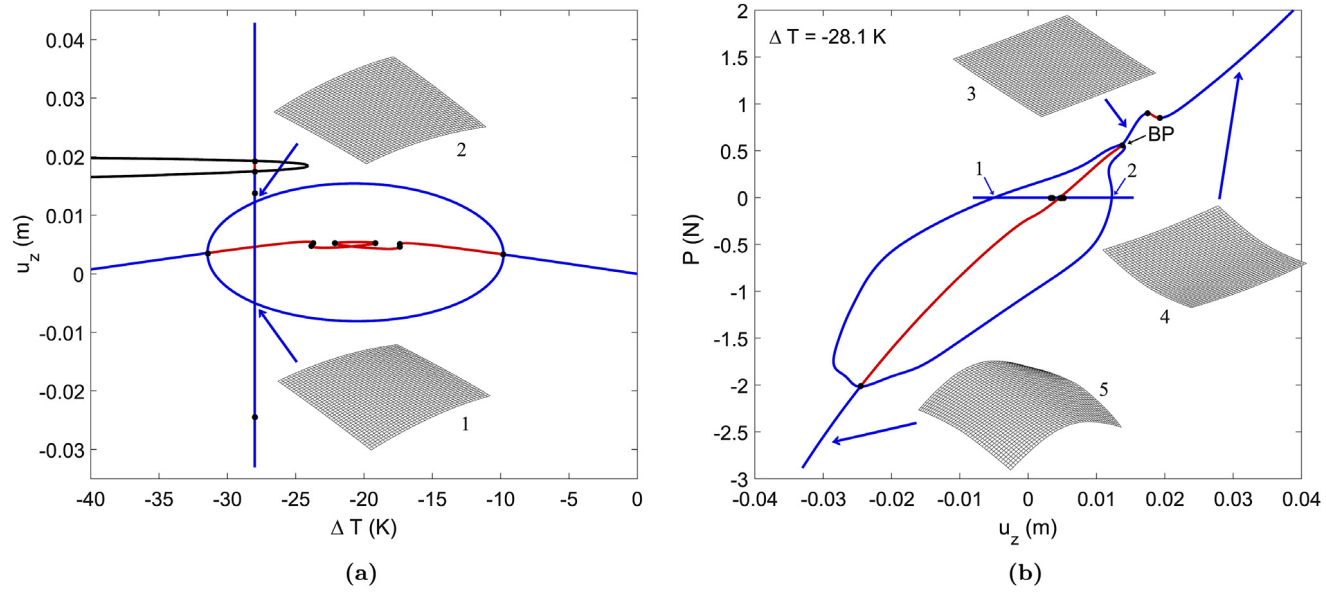

Fig. 5. (a) Close-up view of the twisting-mode portion of the cool-down manifold for $P = 0$ in the temperature (ΔT) *vs* corner displacement (u_z) plane with an orthonormal projection of the foldline in black. The vertical line illustrates the application of corner forces P to snap the laminate between the twisted modes 1 and 2, and beyond. (b) The snap-through manifold in the corner displacement (u_z) *vs* corner force (P) plane between the two twisted modes (1 and 2) and beyond to other modes 3–5.

points (maximum and minimum) on the snap-through manifold with respect to changes in temperature. The projections of this curve onto the temperature (ΔT) *vs* corner force (P) and temperature (ΔT) *vs* corner displacement (u_z) planes are also illustrated for clarity. The mapping of the foldline onto the parameter plane (ΔT *vs* P) clearly shows a cusp catastrophe at $\Delta T = -24.1$ K, *i.e.* the codimension-2 singularity of coincident maxima and minima limit points.

Following the classification of Danso & Karpov [35] published in this journal, the location of the cusp singularity and stability boundary on the broken-away manifold can be used to split the behaviour of the shell into different regions. Fig. 4b shows the broken-pitchfork manifold and the foldline in the ΔT *vs* u_z plane with the following sub-divisions:

- Bistability: for $\Delta T = [-180, -89.4]$ K the shell is bistable and can be snapped between two cylindrical shapes by traversing a region of instability.
- Super-elastic monostability: for $\Delta T = [-89.4, -31.5]$ K the shell can be snapped between two cylindrical shapes but the second state is not self-equilibrated. Hence, if the corner forces are removed, the shell will snap back to its primary cylindrical shape.
- Bistability with additional super-elastic behaviour: for $\Delta T = [-31.5, -24.1]$ K the shell is bistable and can be

snapped between two self-equilibrated twisted shapes. Additionally, for higher values of the corner forces, the shell can also be snapped between a flat and a cylindrical shape. These two shapes are not self-equilibrated, and hence the shell snaps into a twisted shape if the corner forces are removed.
- Bistability: for $\Delta T = [-24.1, -9.79]$ K the shell can be snapped between the two twisted shapes.

The third point above is rather unusual and warrants further examination. Fig. 5a shows a close-up view of the bistable and super-elastic regions in the ΔT *vs* u_z plane with a vertical snap-through curve (u_z *vs* P) at $\Delta T = -28.1$ K. The plot clearly shows how the black foldline splits the snap-through curve into stable and unstable regions. Hence, at this temperature of $\Delta T = -28.1$ K, we can expect bistable behaviour between the two self-equilibrated mode shapes 1 and 2, and additionally, super-elastic behaviour delimited by the foldline.

The snap-through manifold in the orthogonal u_z *vs* P plane is shown in Fig. 5b. The points 1 and 2 marked there correspond to the self-equilibrated twisted shapes shown in Fig. 5a. Thus, as the shell is loaded from point 1 via positive corner forces (P), it smoothly transitions towards the second mode 2 until it reaches the branching point BP. If the loading direction can be reversed at this point while increasing the corner displacement, then the shell will smoothly transition into the second twisted mode 2. Alternatively, if the load is increased beyond BP, then the shell smoothly transitions onto the path corresponding to the flat shape 3. If the load is now removed in this flat state, then the shell naturally snaps into the second twisted shape at point 2. However, if the load P is increased further, then the equilibrium manifold reaches the first limit point lying on the black foldline in Fig. 5a. This causes the shell to traverse the region of instability by snapping into the cylindrical shape 4. Finally, the equilibrium manifold in Fig. 5b shows that the connection between the two twisted shapes 1 and 2 exists through a connection of negative applied corner force as well. Starting at 1, negative corner forces can be applied, and in this case, a different branch point will be encountered that immediately transitions the shell into a different cylindrical shape 5.

Fig. 5 therefore shows a quite unique stability behaviour. Two connected pitchfork bifurcations exists both in the ΔT *vs* u_z plane (Fig. 5a) and in the u_z *vs* P plane (Fig. 5a) to create a closed hull-shaped manifold of stable equilibria intersected by four manifolds, which are stable outside of the closed hull and unstable within. Overall, this creates interesting possibilities for shape adaptation since the shell can be reconfigured between two twisted, two cylindrical, and a flat configuration depending on the combination of applied temperature and corner forces.

3.2. Rectangular shell

For the rectangular shell, the straight length is doubled from $L = 250$ mm to $L = 500$ mm and the laminate stacking sequence reversed. The cool-down behaviour of the laminate from curing to room temperature, $\Delta T = [-180, 0]$, is shown in Fig. 6a. This plot of ΔT *vs* u_z shows the familiar shape of a broken pitchfork, but in this case branching to a twisted mode, which was observed for the square panel, does not occur. Hence, the fundamental path of this broken-pitchfork manifold describes increasing curvature in the direction of the original tool plate (see mode shape I). The broken-away path of the pitchfork is once again stable until a branching point and a closely spaced limit point appear around $\Delta T = -48.3$ K. This stable branch relates to the inverted and 90 deg-rotated mode shape IV. This stable path is slightly obscured in Fig. 6a by the mostly unstable bifurcation path, which branches from the branching point at $\Delta T = -48.3$ K. Inset B shows the two separate equilibrium paths more clearly.

In fact, insets A–C show a narrow band of stable equilibria for $\Delta T = [-146.101, -146.077]$ on this otherwise unstable bifurcation path. In this temperature range the shell has four self-equilibrated stable states, such that the laminate is "quadristable". The vertical dashed line at $\Delta T = -146.1$ K intersects this narrow temperature band and shows the four stable mode shapes I–IV. Apart from the two cylindrical mode shapes I and IV, two additional mode shapes II and III exist that are curved in one direction over half of the laminate length and curved orthogonally over the other half. This shape is familiar in the unrolling or bending of a carpenter's tape [36]. Note that imperfections in practise could easily erode the narrow band of stability. In future work we intend to increase the narrow stable region by tracing the two limiting points (maximum and minimum) in parameter space. In this manner, the combination of geometric and constitutive parameters that maximise the temperature band of four self-equilibrated states can be determined, making it more robust to imperfections.

When the laminate is loaded at $\Delta T = -146.1$ K from mode shape I via the corner forces P, it snaps into mode shape IV. Indeed, preliminary analyses (not shown graphically here) suggest that mode shapes II and III cannot be obtained by the simple imposition of corner forces from either mode shape I or IV. Hence, additional shape control, *e.g.* via additional forces, is needed to take advantage of these additional self-equilibrated mode shapes for morphing applications. Because mode shapes II and III are disconnected from I or IV we do not show the corner displacement (u_z) *vs* corner force (P) equilibrium diagram here. Instead, Fig. 6b shows the snap-through diagram of applied corner force (P) *vs* corner deflection (u_z) from mode shape I to mode shape IV at room temperature ($\Delta T = -180$ K). In both directions, snap-through and snap-back, the laminate loses stability at a branching point and not the maximum/minimum limit points (see inset A). Pirrera et al. [22] previously surmised that the unusual shape of this snap-through equilibrium manifold (explored by these authors in Abaqus without recourse to robust continuation algorithms) is a numerical abberation caused by accidental branch switching. The results here show that this is not the case, and consequently, that the analytical model developed by Pirrera et al. [22] fails to capture the snapping behaviour of this laminate accurately. The bifurcation path branching from this first branching point is also shown in Fig. 6b (unstable segments in grey and stable segments in blue), and displays an interesting destabilising–restabilising behaviour similar to cellular buckling [37]. As shown in inset B, the laminate destabilises and restabilises at consecutive limit points, with the minima preceded and the maxima followed by additional branching points. This cellular buckling behaviour is interesting from a phenomenological point of view, and additionally the isolated regions of stability could be used as an intermediate mode between the two cylindrical shapes I and IV for shape-morphing applications. In this case, additional control points would be needed to guide the laminate into one of these states for a specific value of applied corner force P.

4. Conclusions

This paper revisits two examples from the morphing literature of fibre-reinforced composite laminates [22,24], which are often used to illustrate the bistability of these structures. The nonlinear interaction between initial curvature, differential free thermal strains and slippage constraints between orthotropic layers can lead to "extreme" mechanics of complex branching and multi-stable behaviour. By means of generalised path-following techniques, this work has shown possible snapping behaviour between five different mode shapes (two twisted, two cylindrical and one flat) for different combinations of applied temperature and mechanical loading. Furthermore, for a very small temperature

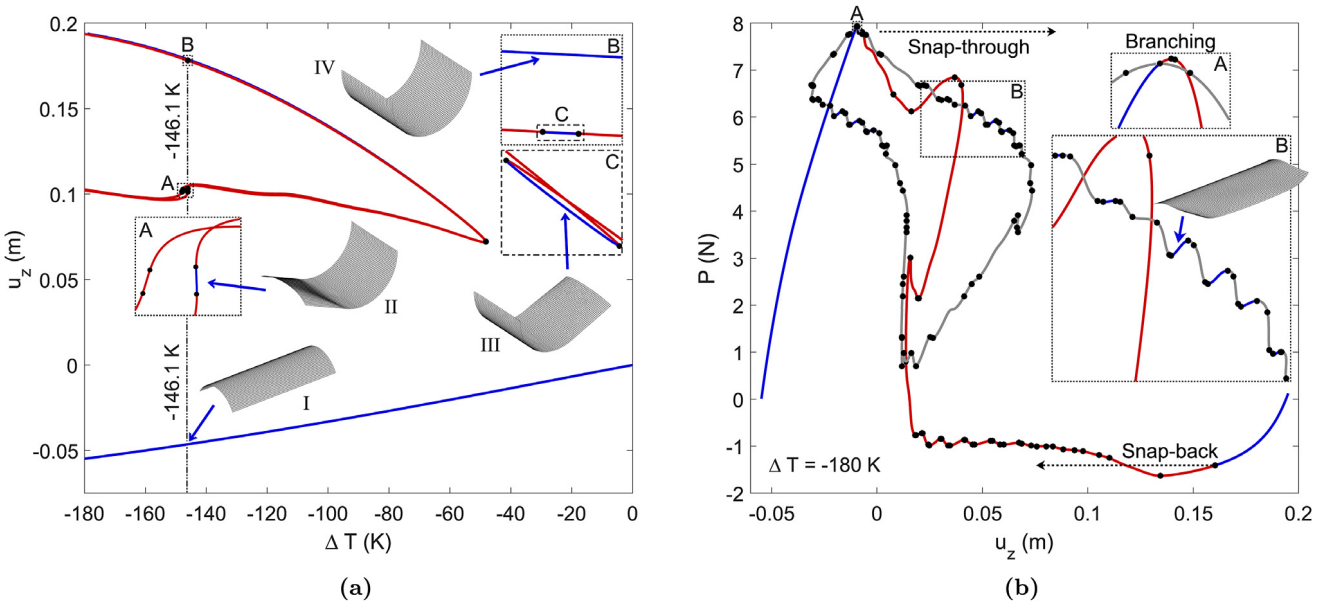

Fig. 6. (a) Broken pitchfork diagram showing the cooling behaviour of a cylindrically cured cross-ply laminate $[0_2/90_2]$ of rectangular planform with mode shapes shown at different points throughout the cooling temperature range. Note the additional stable regions in insets A–C. (b) The snap-through manifold in the corner displacement (u_z) *vs* corner force (P) plane between the two cylindrical modes (I and IV). Note the destabilising/restabilising behaviour on one of the bifurcation paths in inset B. (For interpretation of the references to colour in this figure legend, the reader is referred to the web version of this article.)

range, a cylindrical laminate of rectangular planform may be self-equilibrated in four different shapes. The present findings show that composite laminates can exhibit a much richer nonlinear behaviour than previously assumed, and this may influence the design of more versatile shape-adaptive structures.

Generalised path-following provides a systematic approach of determining critical points while path-following and branching onto additional connected equilibrium paths. As shown here, this greatly improves our ability to explore the stability landscape. However, when additional equilibrium paths exist that are broken-away from known solutions (as is likely for the multistable systems studied here), it can be challenging to find these. Specific strategies, such as the branch-connecting paths outlined in Ref. [12], can be used to "search" for additional equilibria and this promises to be a fruitful avenue for further research.

While the twisting modes of the "square" shell have been shown experimentally [24], the other stable states described here are more difficult to validate experimentally as additional control points are needed to guide the laminate into these alternative stable states. Hence, our work also aims to provide impetus for the development of new testing methods that are particularly suited to validating and certifying multistable morphing structures. One potential approach is global *shape control* of the structure and this is currently being pursued by the present authors [13].

Acknowledgements

RMJG is supported by the Royal Academy of Engineering under the Research Fellowship scheme [Grant No. RF\201718\17178], and AP is supported by the EPSRC through the Early-Career Fellowship scheme [Grant No. EP/M013170/1].

Data statement

All data required to reproduce the figures in this paper are available at the University of Bristol data repository, *data.bris*, at https://doi.org/10.5523/bris.233dw35gj5opw2mjm8tdr7sbn0.

References

[1] N. Hu, R. Burgueño, Buckling-induced smart applications: recent advances and trends, Smart Mater. Struct. 24 (2015) 063001.
[2] R.L. Harne, K.W. Wang, A review of the recent research on vibration energy harvesting via bistable systems, Smart Mater. Struct. 22 (2013) 023001.
[3] S. Emam, D. Inman, A review on bistable composite laminates for morphing and energy harvesting, Appl. Mech. Rev. 67 (6) (2015) 060803.
[4] G. Arena, R.M.J. Groh, A. Brinkmeyer, R. Theunissen, P.M. Weaver, A. Pirrera, Adaptive compliant structures for flow regulation, Proc. R. Soc. Lond. Ser. A Math. Phys. Eng. Sci. 473 (2017) 20170334.
[5] M. Gomez, D.E. Moulton, D. Vella, Passive control of viscous flow via elastic snap-through, Phys. Rev. Lett. 119 (2017) 144502.
[6] K.A. Seffen, S.V. Stott, Surface texturing through cylinder buckling, J. Appl. Mech. 81 (2014) 061001.
[7] J.T.B. Overvelde, T. Kloek, J.J.A. D'haen, K. Bertoldi, Amplifying the response of soft actuators by harnessing snap-through instabilities, Proc. Natl. Acad. Sci. 112 (35) (2015) 10863–10868.
[8] J. Shim, C. Perdigou, R.E. Chen, K. Bertoldi, P.M. Reis, Buckling-induced encapsulation of structured elastic shells under pressure, Proc. Natl. Acad. Sci. 109 (16) (2012) 5978–5983.
[9] K. Bertoldi, P.M. Reis, S. Willshaw, T. Mullin, Negative Poisson's ratio behavior induced by an elastic instability, Adv. Mater. 22 (2010) 361–366.
[10] N. Hu, R. Burgueño, Tailoring the elastic postbuckling response of cylindrical shells: A route for exploiting instabilities in materials and mechanical systems, Extreme Mech. Lett. 4 (2015) 103–110.
[11] N. Hu, R. Burgueño, Elastic postbuckling response of axially-loaded cylindrical shells with seeded geometric imperfection design, Thin-Walled Struct. 96 (2015) 256–268.
[12] R.M.J. Groh, D. Avitabile, A. Pirrera, Generalised path-following for well-behaved nonlinear structures, Comput. Methods Appl. Mech. Engrg. 331 (2018) 394–426.
[13] R.M. Neville, R.M.J. Groh, A. Pirrera, M. Schenk, Shape control for experimental continuation, Phys. Rev. Lett. 120 (2018) 254101.
[14] J. Sun, Q. Guan, Y. Liu, J. Leng, Morphing aircraft based on smart materials and structures: A state-of-the-art review, J. Intell. Mater. Syst. Struct. 27 (17) (2016) 2289–2312.
[15] B.C. Kim, K. Potter, P.M. Weaver, Continuous tow shearing for manufacturing variable angle tow composites, Composites A 43 (2012) 1347–1356.
[16] M.W. Hyer, Some observations on the cured shape of thin unsymmetric laminates, J. Compos. Mater. 15 (1981) 175–194.
[17] B.H. Coburn, A. Pirrera, P.M. Weaver, S. Vidoli, Tristability of an orthotropic doubly curved shell, Compos. Struct. 96 (2013) 446–454.
[18] C. Thill, J. Etches, I. Bond, K. Potter, P.M. Weaver, Morphing skins, Aeronaut. J. 112 (2008) 117–139.
[19] M.L. Dano, M.W. Hyer, Thermally-induced deformation behavior of unsymmetric laminates, Int. J. Solids Struct. 35 (17) (1998) 2101–2120.

[20] S. Vidoli, C. Maurini, Tristability of thin orthotropic shells with uniform initial curvature, Proc. R. Soc. Lond. Ser. A Math. Phys. Eng. Sci. 464 (2008) 2949–2966.
[21] S.D. Guest, S. Pellegrino, Analytical models for bistable cylindrical shells, Proc. R. Soc. Lond. Ser. A Math. Phys. Eng. Sci. 462 (2006) 839–854.
[22] A. Pirrera, D. Avitabile, P.M. Weaver, On the thermally induced bistability of composite cylindrical shells for morphing structures, Int. J. Solids Struct. 49 (2012) 685–700.
[23] M. Schlecht, K. Schulte, Advanced calculation of the room-temperature shapes of unsymmetric laminates, J. Compos. Mater. 33 (16) (1999) 1472–1490.
[24] E. Eckstein, A. Pirrera, P.M. Weaver, Multi-mode morphing using initially curved composite plates, Compos. Struct. 109 (2014) 240–245.
[25] H.B. Keller, Lectures on Numerical Method in Bifurcation Problems, Tata Institute of Fundamental Research, 1986.
[26] E.L. Allgower, K. Georg, Continuation and path following, Acta Numer. (1992) 1–64.
[27] E.J. Dödel, A.R. Champneys, T.F. Fairgrieve, Y.A. Kuznetsov, B. Sandstede, X. Wang, AUTO 97: Continuation and Bifurcation software for ordinary differential equations (with HomCont), 1998.
[28] E. Riks, An incremental approach to the solution of snapping and buckling problems, J. Solids Struct. 15 (1979) 529–551.
[29] S. Ahmad, B.M. Irons, O.C. Zienkiewicz, Analysis of thick and thin shell structures by curved finite elements, Internat. J. Numer. Methods Engrg. 2 (1970) 419–451.
[30] E. Reissner, On the theory of bending of elastic plates, J. Math. Phys. 23 (1944) 184–191.
[31] E. Ramm, A plate/shell element for large deflections and rotations, in: Formulations and Computational Algorithms in Finite Element Analysis, MIT Press, Cambridge, MA, USA, 1977.
[32] S. Daynes, C.G. Diaconu, K.D. Potter, P.M. Weaver, Bistable prestressed symmetric laminates, J. Compos. Mater. 44 (9) (2010) 1119–1137.
[33] E. Eckstein, A. Pirrera, P.M. Weaver, Morphing high-temperature composite plates utilizing thermal gradients, Compos. Struct. 100 (2013) 363–372.
[34] S. Armon, E. Efrati, R. Kupferman, E. Sharon, Geometry and mechanics in the opening of chiral seed pods, Science 333 (2011) 1726–1730.
[35] L.A. Danso, E.G. Karpov, Cusp singularity-based bistability criterion for geometrically nonlinear structures, Extreme Mech. Lett. 13 (2017) 135–140.
[36] K.A. Seffen, S. Pellegrino, Deployment dynamics of tape springs, Proc. R. Soc. Lond. Ser. A Math. Phys. Eng. Sci. 455 (1999) 1003–1048.
[37] G.W. Hunt, M.A. Peletier, A.R. Champneys, P.D. Woods, M.A. Wadee, C.J. Budd, G.J. Lord, Cellular buckling in long structures, Nonlinear Dynam. 21 (2000) 3–29.